Surface Composition of Carbon Nanotubes-Fe-Alumina Nanocomposite Powders: An Integral Low-Energy Electron Mo1ssbauer Spectroscopic Study

Valdirene Gonzaga de Resende, Eddy de Grave, Alain Peigney, Christophe Laurent

▶ **To cite this version:**

Valdirene Gonzaga de Resende, Eddy de Grave, Alain Peigney, Christophe Laurent. Surface Composition of Carbon Nanotubes-Fe-Alumina Nanocomposite Powders: An Integral Low-Energy Electron Mo1ssbauer Spectroscopic Study. Journal of Physical Chemistry C, 2008, 112 (15), pp.5756-5761. ⟨10.1021/jp711679w⟩. ⟨hal-03578175⟩

HAL Id: hal-03578175

https://hal.science/hal-03578175v1

Submitted on 17 Feb 2022

HAL is a multi-disciplinary open access archive for the deposit and dissemination of scientific research documents, whether they are published or not. The documents may come from teaching and research institutions in France or abroad, or from public or private research centers.

L'archive ouverte pluridisciplinaire **HAL**, est destinée au dépôt et à la diffusion de documents scientifiques de niveau recherche, publiés ou non, émanant des établissements d'enseignement et de recherche français ou étrangers, des laboratoires publics ou privés.

HAL Authorization

Open Archive Toulouse Archive Ouverte (OATAO)
OATAO is an open access repository that collects the work of Toulouse researchers and makes it freely available over the web where possible.

This is an author-deposited version published in: http://oatao.univ-toulouse.fr/
Eprints ID : 2637

To link to this article :
URL : http://dx.doi.org/10.1021/jp711679w

To cite this version : De Resende, V.G and De Grave, E. and Peigney, Alain and Laurent, Christophe (2008) *Surface Composition of Carbon Nanotubes-Fe-Alumina Nanocomposite Powders: An Integral Low-Energy Electron Mo1ssbauer Spectroscopic Study.* Journal of Physical Chemistry C, vol. 112 (n° 15). pp. 5756-5761. ISSN 1932-7447

Any correspondence concerning this service should be sent to the repository administrator: staff-oatao@inp-toulouse.fr

Surface Composition of Carbon Nanotubes-Fe-Alumina Nanocomposite Powders: An Integral Low-Energy Electron Mössbauer Spectroscopic Study

Valdirene G. de Resende,*,† Eddy De Grave,† Alain Peigney,‡ and Christophe Laurent‡

Department of Subatomic and Radiation Physics, University of Ghent, B-9000 Gent, Belgium, and CIRIMAT, CNRS/UPS/INPT, LCMIE, Université Paul-Sabatier, Bât. 2R1, 118 route de Narbonne, 31062 Toulouse cedex 9, France

The surface state of carbon nanotubes-Fe-alumina nanocomposite powders was studied by transmission and integral low-energy electron Mössbauer spectroscopy. Several samples, prepared under reduction of the α-$Al_{1.8}Fe_{0.2}O_3$ precursor in a H_2-CH_4 atmosphere applying the same heating and cooling rate and changing only the maximum temperature (800−1070 °C) were investigated, demonstrating that integral low-energy electron Mössbauer spectroscopy is a promising tool complementing transmission Mössbauer spectroscopy for the investigation of the location of the metal Fe and iron-carbide particles in the different carbon nanotube−nanocomposite systems containing iron. The nature of the iron species (Fe^{3+}, Fe_3C, α-Fe, γ-Fe−C) is correlated to their location in the material. In particular, much information was derived for the powders prepared by using a moderate reduction temperature (800, 850, and 910 °C), for which the transmission and integral low-energy electron Mössbauer spectra are markedly different. Indeed, α-Fe and Fe_3C were not observed as surface species, while γ-Fe−C is present at the surface and in the bulk in the same proportion independent of the temperature of preparation. This could show that most of the nanoparticles (detected as Fe_3C and/or γ-Fe−C) that contribute to the formation of carbon nanotubes are located in the outer porosity of the material, as opposed to the topmost (ca. 5 nm) surface. For the higher reduction temperatures T_r of 990 °C and 1070 °C, all Fe and Fe-carbide particles formed during the reduction are distributed evenly in the bulk and the surface of the matrix grains. The integral low-energy electron Mössbauer spectroscopic study of a powder oxidized in air at 600 °C suggests that all Fe_3C particles oxidize to α-Fe_2O_3, while the α-Fe and/or γ-Fe−C are partly transformed to $Fe_{1-x}O$ and α-Fe_2O_3, the latter phase forming a protecting layer that prevents total oxidation.

Introduction

Since their discovery by Iijima,[1] carbon nanotubes have been one of the most actively studied materials in nowadays' research. In a recent listing of most popular subjects in physics research,[2] carbon nanotubes are first. This widely spread interest is explained by the potential extraordinary technological applications of this material. Among the many possible application fields are ceramic-matrix nanocomposites containing carbon nanotubes.[3] One of the main hurdles for the successful preparation of such composites is to obtain a homogeneous distribution of undamaged carbon nanotubes into the matrix. To overcome the need for a mechanical-mixing step during powder preparation, a direct method for the in situ synthesis of the carbon nanotube into an Al_2O_3 matrix has been proposed.[4] It is based on a catalytic chemical vapor deposition route involving the reduction in H_2-CH_4 gas atmosphere of alumina-hematite solid solutions, producing carbon nanotubes-Fe−Al_2O_3 nanocomposite powders. The reduction first produces nanometric Fe particles that are active for the decomposition of CH_4, and subsequently for the formation of carbon nanotubes if their diameter is small enough (< ca. 5 nm).[5,6]

It is well-known that ^{57}Fe Mössbauer spectroscopy offers several advantages for studies of iron-containing compounds. The spectra and parameters derived from these are very sensitive to electronic, magnetic, and structural characteristics of the probed material, and as such, Mössbauer spectroscopy is a useful tool for phase identification and quantification of mixtures of Fe-bearing solid materials. Although Fe species are often involved in carbon nanotube formation processes, only relatively few carbon nanotube-related studies, apart from those by some of the present authors,[6−16] report on Mössbauer data with regard to the formation, evolution, and the spatial distribution of Fe-containing particles after synthesis of the carbon nanotubes by catalytic chemical vapor deposition methods.[17−20] Furthermore, some authors reported on the characterization by Mössbauer spectroscopy of metal-filled carbon nanotubes.[21−27] Finally, Mössbauer spectroscopy was applied in the characterization of carbon nanotubes decorated with iron oxides.[28,29]

In a previous work,[6] carbon nanotubes-Fe−Al_2O_3 nanocomposite powders were prepared by the H_2-CH_4 reduction of α-$Al_{1.8}Fe_{0.2}O_3$ at different temperatures. The carbon nanotubes were mostly single and double walled, but thicker carbon nanofibers were also observed. By using several characterization techniques including conventional transmission Mössbauer spectroscopy, several iron species were detected in the nanocomposite powders: Fe^{3+} ions still present in the α-alumina lattice, α-Fe, γ-Fe−C, and cementite (Fe_3C). Three major

* To whom correspondence should be addressed. Fax: +32-(0)9-264-6697. E-mail: Valdirene.Gonzaga@Ugent.be.
† University of Ghent.
‡ Université Paul-Sabatier.

10.1021/jp711679w

conclusions were inferred: (i) the γ-Fe−C particles are embedded inside the matrix grains, (ii) the cementite particles are on the surface of the matrix grains, and (iii) the α-Fe particles are found both inside and on the surfaces of the grains. It was further proposed that the nanoparticles responsible for the formation of carbon nanotubes ended up as Fe_3C after cooling down from the selected temperature (T_r).

In the present work, the authors for the first time have studied the surface of these powders by integral low-energy electron Mössbauer spectroscopy. This technique is a variant of transmission Mössbauer spectroscopy in which low-energy electrons are counted. These electrons, with energy of ∼10 eV, are produced by after effects following the decay of the probe nuclei in the absorber. As a consequence of this low energy, only an extremely thin surface layer (about 5 nm) of the material is probed.[30] It was the intention using this unique technique to obtain further and sounder information on the spatial distribution of the Fe-bearing particles with respect to the nanocomposite grains.

Experimental Section

The synthesis of the powders and their characterization by X-ray diffraction, carbon element analysis, specific surface area measurements, and transmission and scanning electron microscopy are described in detail elsewhere.[6] Briefly, the carbon nanotubes-Fe−Al_2O_3 nanocomposite powders were prepared by the reduction of α-$Al_{1.8}Fe_{0.2}O_3$ in H_2−CH_4 (18 mol % CH_4) at different temperatures (T_r = 800, 850, 910, 990, and 1070 °C). The heating rate to T_r and the subsequent cooling rate were equal to 5 °C/min, and no dwell time was applied at T_r. The so-obtained nanocomposite powders are designated in the following as R800, R850, R910, R990, and R1070, according to the corresponding T_r.

The powders were observed by field-emission gun-scanning electron microscopy. Mössbauer spectra at room temperature were collected with spectrometers operating in constant acceleration mode with triangular reference signal. ^{57}Co(Rh) sources were used. Both conventional transmission spectra and integral low-energy electron Mössbauer spectra (hereafter referred as emission spectra) have been acquired. All Mössbauer spectra were computer-analyzed in terms of model-independent distributions of hyperfine-parameter values and numerical data quoted hereafter refer to maximum-probability values.[31] Isomer shifts are referenced with respect to α-Fe at room temperature. The line width values were adjusted in the transmission spectra (which were of very high statistical quality), and the adjusted values were then used as fixed parameters for the emission spectra. Average fitted width values for all involved subspectral components were found to be ∼0.30 mm/s.

Results and Discussion

The transmission spectra of the nanocomposite powders are shown in Figure 1 (left) and the corresponding Mössbauer parameters are summarized in Table 1. All spectra have been analyzed with superpositions of model-independent hyperfine-field and quadrupole-splitting distributions. Four components were found to be required to obtain adequate fits for these spectra: (i) an outer sextet showing hyperfine parameters that are characteristic of α-Fe, (ii) an inner sextet that could be attributed to Fe_3C, (iii) an Fe^{3+} doublet due to iron ions present in the lattice of the α-alumina, and (iv) a singlet that corresponds to a γ-Fe phase, possibly alloyed with carbon (γ-Fe−C). No significant differences in parameter values between the presently measured transmission data and those obtained earlier[6] were

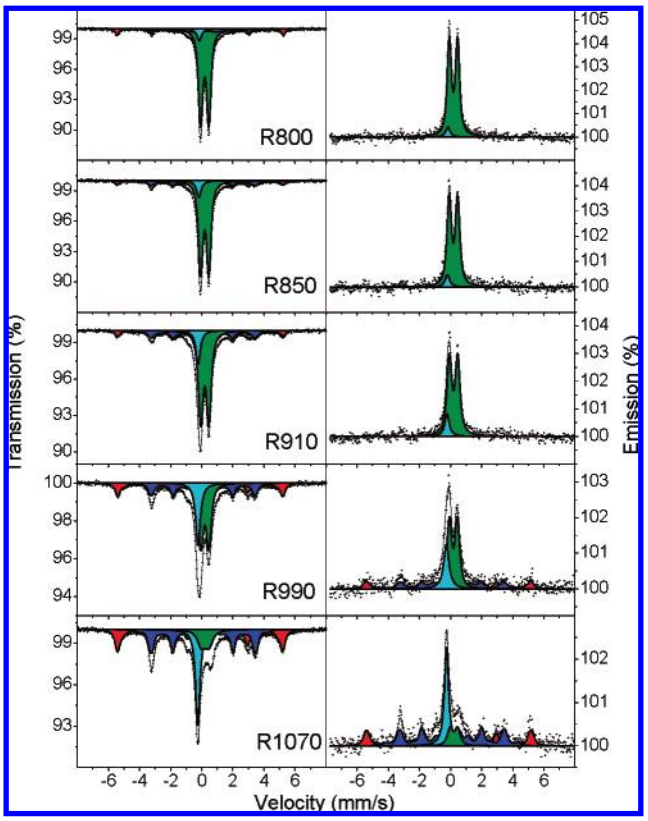

Figure 1. Transmission (left) and emission (right) spectra of the nanocomposites powders measured at room temperature. α-Fe (red); Fe_3C (blue); $(Al,Fe)_2O_3$ (olive); γ-Fe−C (cyan).

observed. Obviously, increasing the temperature of reduction has a major influence on the transmission spectra, in particular, as to the contribution of the central doublet (accounting for Fe^{3+} ions) which decreases considerably with increasing T_r (Figure 2 top and Table 1). This decrease is accounted for by the gradual increase of the other components present in the transmission spectra.

The results of the integral low-energy electron Mössbauer spectroscopic experiments are shown in the right panel of Figure 1. The emission spectra exhibit the same shape as the transmission spectra (Figure 1, left). The fitted hyperfine parameters (Table 1) do not significantly differ from the respective values derived from the transmission spectra. For R990 and R1070, all four iron phases are recognized, however, with slightly different relative spectral areas from those observed in the transmission spectra (Table 1), showing that all species are present in the topmost surface of the grains. Interestingly, the emission spectra of samples R800, R850, and R910 do not show spectral components due to α-Fe and Fe_3C, suggesting that the involved particles are not located at the topmost surface of the alumina grains. The relative spectral area contributions of the γ-Fe−C subspectra to the total spectra are found to be the same in the respective transmission and emission experiments, suggesting that γ-Fe−C particles are evenly distributed between the surface and those deeper in the material. The absence of α-Fe and Fe_3C components in the emission spectra is totally accounted for by the more intense Fe^{3+} doublet in the latter spectra as witnessed by the respective relative spectral area values. These results, in particular, the absence of Fe_3C in the topmost layer, are puzzling because they are partly in contradiction with the earlier conclusions[6] mentioned above.

Field-emission gun-scanning electron microscopy images of selected composite powders are reported in Figure 3. For R800

TABLE 1: Mössbauer Results of the Carbon Nanotubes-Fe-Alumina Nanocomposite Samples Measured at Room Temperature[a]

Transmission Mössbauer Spectroscopy														
	α-Fe				Fe_3C				$(Al,Fe)_2O_3$			γ-Fe−C		
sample	$H_{hf,m}$	$2\epsilon_Q$	*RA*	δ	$H_{hf,m}$	$2\epsilon_Q$	*RA*	δ	$\Delta E_{Q,m}$	*RA*	δ	ΔE_Q	*RA*	δ
R800	33.1	0.00*	9	0.02	21.1	0.03*	13	0.19*	0.53	73	0.30	0.00*	5	−0.05
R850	33.0	0.00*	6	0.01	20.7	0.03*	20	0.19*	0.53	67	0.30	0.00*	7	−0.08
R910	33.2	0.00*	8	0.01	20.8	0.03*	23	0.19	0.53	58	0.31	0.00*	11	−0.12
R990	32.9	0.00*	19	0.02	20.7	0.03*	27	0.19	0.51	36	0.31	0.00*	18	−0.13
R1070	32.9	0.00*	27	0.00	20.8	0.03*	36	0.20	0.48	13	0.33	0.00*	24	−0.14
Integral Low-Energy Electron Mössbauer Spectroscopy														
R800									0.53	94	0.30	0.00*	6	−0.05*
R850									0.53	93	0.30	0.00*	7	−0.08*
R910									0.52	87	0.30	0.00*	13	−0.11
R990	33.0	0.00*	14	−0.01	20.7	0.03*	24	0.19*	0.50	44	0.29	0.00*	18	−0.15
R1070	32.9	0.00*	22	0.00	20.8	0.03*	40	0.20	0.49	11	0.33*	0.00*	27	−0.14

[a] H_{hf}: hyperfine field at maximum of the distribution (T). $2\epsilon_Q$: quadrupole shifts (mm/s). ΔE_Q: quadrupole splitting (mm/s). δ: isomer shifts (mm/s). RA: relative spectral areas (%). The values of isomer shifts are with reference to metallic iron. *Fixed parameters.

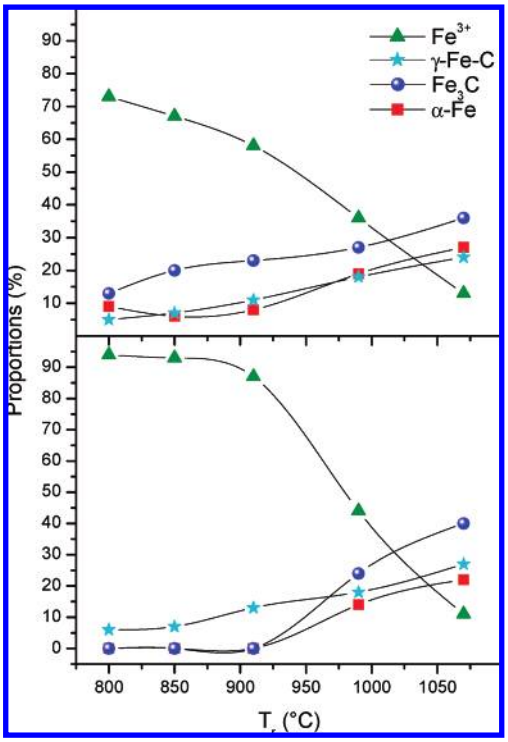

Figure 2. Proportions of the iron phases in the nanocomposite powders as revealed by the transmission (top) and emission (bottom) versus the reduction temperature. The lines are guides for the eye.

(Figure 3a), one observes alumina grains, presenting the vermicular microstructure with large irregular pores, decorated by particles (about 10−20 nm) appearing as light-gray dots, some of which are indicated by arrows on the image. No carbon nanotubes are observed because T_r was rather low (800 °C) for CH_4 decomposition. For R850 (Figure 3b), the same features are observed, but carbon nanotubes are observed as well. Note that the particles observed at the surface of alumina do not appear to be connected to the carbon nanotubes. For R910 and R990 (Figure 3c,d, respectively), the proportion of bundled carbon nanotubes is much more important, and carbon nanofibers are observed as well. Lower magnification images (not shown) reveal that the proportion of carbon nanofibers with respect to carbon nanotubes is not negligible. It was shown by the analysis of the emission spectra of R800, R850, and R910 (Table 1) that α-Fe and Fe_3C particles are not located at the topmost surface of the alumina grains. Thus, the surface particles observed by scanning electron microscopy (Figure 3) are γ-Fe−C. These particles are fairly large, contrary to a previous hypothesis that the γ phase, as opposed to the α phase, was an indication of a very low size. Because there is an increase in the content of carbon nanotubes between R800 and R850 but no marked increase in the γ-Fe−C proportion (Table 1), one could propose that most of the nanoparticles (detected as Fe_3C and/or γ-Fe−C) that contribute to the formation of carbon nanotubes are located in the outer porosity of the material, as opposed to the surface. Particles located in a pore would be less prone to excessive growth than a surface particle would. This is in line with earlier results[5,6] showing that the diameter of the surface particles (about 10−20 nm) is far too high for them to be active for the formation of carbon nanotubes. Indeed, the critical diameter is in the range 3−5 nm, and larger particles either become totally covered by carbon layers or are active for the formation of carbon nanofibers.

In order to gather more information about the location of the different iron phases in the nanocomposite powders, that is, inside the matrix grains, the outer porosity, or on their surfaces, sample R990 was heat-treated in air at 600 °C for 2 h and studied by transmission Mössbauer spectroscopy.[6] Note that this treatment burns all of the carbon nanotubes and carbon nanofibers. The transmission and the emission spectra were collected at room temperature for this sample designated R990ox600 in the following (Figure 4). The hyperfine parameters obtained from the fits of the spectra are listed in Table 2. In contrast to the transmission, the emission spectrum is composed of only four components (instead of five) which are: (i) a sextet with hyperfine parameters characteristic of hematite (α-Fe_2O_3), (ii) a singlet due to γ-Fe−C, (iii) an Fe^{3+} doublet attributed to the nonreacted alumina-based solid solution, and (iv) a second broad and less intense doublet that resembles the doublet in the aforementioned transmission spectrum and which has been suggested to arise from an $FeAl_2O_4$ phase.[6] The α-alumina Fe^{3+}, the α-Fe_2O_3, and the γ-Fe−C components represent similar contributions in both the transmission and the emission spectra, while the broad doublet component is considerably more abundant in the emission spectrum (Table 2). The transmission spectrum showed, in addition to the phases mentioned above, a contribution due to α-Fe particles (relative spectral area ∼8%; see Table 2). Interestingly, cementite is not detected in the transmission nor in the emission spectrum, showing that these particles have entirely been oxidized and thus that they were easily accessible to the oxidizing atmosphere, whether they were located in the outer porosity and/or at the surface of the alumina grains. The Fe^{3+} doublet represents the iron ions that were still present in the lattice of α-alumina after

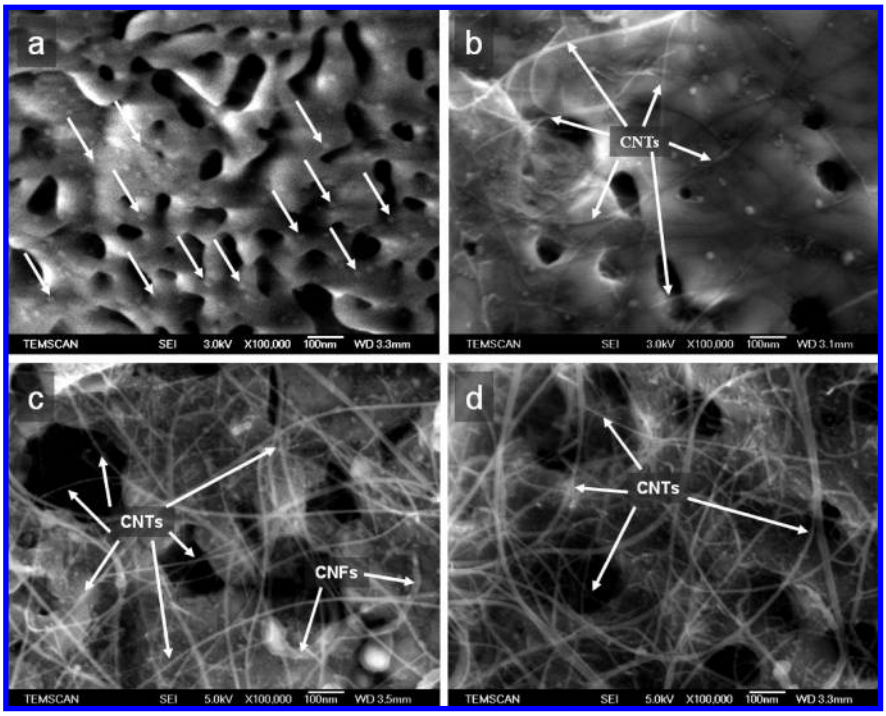

Figure 3. Field-emission gun-scanning electron microscopy images of nanocomposite powders: R800 (a), R850 (b), R910 (c), and R990 (d). CNTs, carbon nanotubes; and CNFs, carbon nanofibers.

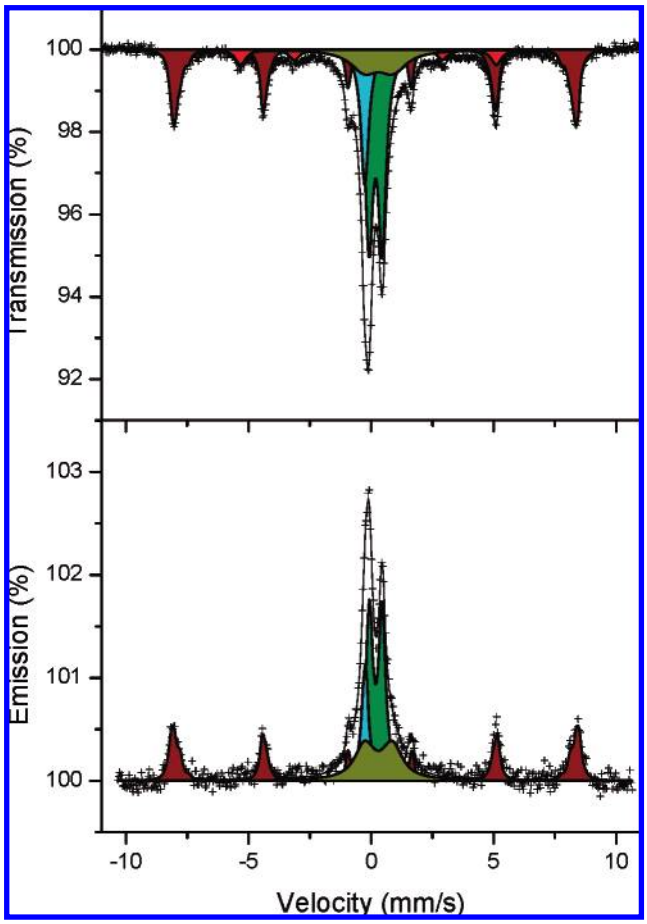

Figure 4. Transmission (top) and emission (bottom) spectra collected at room temperature of sample R990 oxidized at 600 °C in air. α-Fe_2O_3 (wine); α-Fe (red); $(Al,Fe)_2O_3$ (olive); γ-Fe−C (cyan); doublet (dark yellow).

the reduction step (i.e., for specimen R990), which of course are not affected by the oxidation in air. Comparing the relative contributions (relative spectral area; Table 2) could indicate that the hematite particles are formed by the oxidation of cementite. This is consistent with the findings reported by Dong et al.[32] on the basis of thermal analysis of synthetic cementite.

No α-Fe is detected in the emission spectrum, which could indicate that most α-Fe particles remaining in the R900ox600 specimen are in intragranular position. This is in agreement with previous findings[33] showing that intragranular metal particles in similar carbon-free metal−Al_2O_3 powders do not oxidize in flowing air below about 800 °C. The surface α-Fe particles were thus oxidized into species that could contribute to the broad doublet component. It could also be proposed that the γ-Fe−C particles that did not oxidize (about 70% of the population) were the larger ones and/or those covered by many carbon layers, whereas those that were less protected oxidized into species that could contribute to the broad doublet component. With regard to the formation of the $FeAl_2O_4$ phase, it implies that α-Fe and γ-Fe−C particles would have reacted with the alumina matrix grains during the oxidation step. However, one can argue that the broad doublet, suggested[6] to be due to that phase, actually is representative for another Fe-containing oxide. The adjusted values for the quadrupole splittings and isomer shifts are indeed drastically deviating from those found for synthetic $FeAl_2O_4$.[34] Identification of the precise nature of the Fe phase on the basis of the adjusted doublet parameters is, however, not possible because of the strong overlap of the weak and broad doublet lines with the other absorption/emission lines present in the central part of the spectra and hence the ill-defined values of the hyperfine parameters of the doublet. It is not unreasonable that the doublet can be attributed to wustite, $Fe_{1-x}O$, that may indeed form under the conditions applied in the present oxidation experiments.[35] It is well-known that iron particles in general actively react with oxygen even at room temperature, resulting in an iron oxide layer on the surface of the particles. The formation of these oxide layers can protect the particles against further inward oxidation. Fung et al.[36] have reported the remarkable resistance against oxidation of passivated nanopar-

TABLE 2: Mössbauer Results at Room Temperature of Sample R990ox600[a]

Transmission Mössbauer Spectroscopy															
α-Fe_2O_3				α-Fe				$(Al,Fe)_2O_3$			γ-Fe−C		doublet		
$H_{hf,m}$	$2\epsilon_Q$	*RA*	δ	H_{hf}	$2\epsilon_Q$	*RA*	δ	ΔE_Q	*RA*	δ	*RA*	δ	$\Delta E_{Q,m}$	*RA*	δ
50.9	−0.19	30	0.36	32.3	0.0*	8	0.0*	0.54	36	0.30	13	−0.14	1.13	13	0.42
Integral Low-Energy Electron Mössbauer Spectroscopy															
51.0	−0.19	29	0.37					0.52	36	0.30	13	−0.13	1.08	22	0.41

[a] H_{hf}: hyperfine field at maximum of the distribution (T). $2\epsilon_Q$: quadrupole shift (mm/s). ΔE_Q: quadrupole splitting (mm/s). δ: isomer shift (mm/s). RA: relative spectral area (%). The values of isomer shifts are with reference to metallic iron. *Fixed parameters.

ticles of α-Fe, which they claim to be due to a sufficiently thick shell of γ-Fe_2O_3 (4 nm). Other authors characterized α-Fe nanoparticles prepared by sputtering method and subsequently covered with a protective nanocrystalline oxide shell composed of either maghemite (γ-Fe_2O_3) or partially oxidized magnetite (Fe_3O_4).[37] Cui et al.[38] have reported on the oxidation behavior of nanoparticles of Fe prepared by the hydrogen arc plasma method. The authors demonstrated by transmission electron spectroscopic images that the oxidation of these particles in air at temperatures below 600 °C provokes the formation of lighter cores and darker outer shells, the latter disappearing for oxidation temperatures exceeding 600 °C. As observed from X-ray diffraction, the composite particles after oxidation at low temperature (<600 °C) consist of α-Fe_2O_3, γ-Fe_2O_3, and α-Fe. As a result of the phase transformation from γ- to α-Fe_2O_3, only the hematite phase is present at above 600 °C. By considering the above observations and combining the transmission and emission results for sample R990ox600, it is tempting to suggest that the thermal treatment in air caused the surface α-Fe and/or γ-Fe−C (or a fraction of them) to be partly transformed to $Fe_{1-x}O$ and α-Fe_2O_3, the latter phase forming a protecting layer that prevents total oxidation. Thus, some surface particles are not monophased, and the assumption[6] that a given iron-species in specimen R990 was oxidized into another well-defined iron species was too simple.

Conclusions

The study of carbon nanotubes-Fe-alumina nanocomposite powders by integral low-energy electron Mössbauer spectroscopy has given detailed information about the surface state of the powders, demonstrating that this technique is a promising tool complementing transmission Mössbauer spectroscopy for the investigation of the location of the metal Fe and iron-carbide particles in the different carbon nanotubes−nanocomposite systems containing iron. In particular, much information was derived for the powders prepared by using a moderate reduction temperature (800, 850, and 910 °C), for which the transmission and emission spectra are markedly different. Indeed, α-Fe and Fe_3C were not observed as surface species, while γ-Fe−C was present at the surface and in the bulk in the same proportion independent of the temperature of preparation. This could show that most of the nanoparticles (detected as Fe_3C and/or γ-Fe−C) that contribute to the formation of carbon nanotubes are located in the outer porosity of the material, as opposed to the surface. A location in a pore would prevent excessive growth more efficiently than a location on the surface. The integral low-energy electron Mössbauer spectroscopic study of a powder oxidized in air at 600 °C suggests that all Fe_3C particles oxidize to α-Fe_2O_3, while the α-Fe and/or γ-Fe−C are partly transformed to $Fe_{1-x}O$ and α-Fe_2O_3, the latter phase forming a protecting layer that prevents total oxidation. Thus, some surface particles are not monophased after oxidation.

Acknowledgment. This work was partially funded by the Fund for Scientific Research − Flanders, and by the Special Research Fund (BOF, Bijzonder Onderzoeksfonds), UGent (B/06633), Belgium.

References and Notes

(1) Iijima, S. *Nature* **1991**, *354*, 56.
(2) http://physicsweb.org/articles/news/10/5/4.
(3) Peigney, A.; Laurent, Ch. In *Ceramic Matrix Composites: Microstructure, Properties and Applications*; Low, I. M., Ed.; Woodhead Publishing Ltd, Cambridge, 2006; 309−333.
(4) Peigney, A.; Laurent, Ch.; Dobigeon, F.; Rousset, A. *J. Mater. Res.* **1997**, *12*, 613.
(5) Hafner, J. A.; Bronikowski, M. J.; Azamian, B. R.; Nikolaev, P.; Rinzler, A. G.; Colbert, D. T.; Smith, K. A.; Smalley, R. E. *Chem. Phys. Lett.* **1998**, *296*, 195.
(6) Peigney, A.; Coquay, P.; Flahaut, E.; Vandenberghe, R. E.; De Grave, E.; Laurent, Ch. *J. Phys. Chem. B* **2001**, *105*, 9699.
(7) Laurent, Ch.; Peigney, A.; Rousset, A. *J. Mater. Chem.* **1998**, *8*, 1263.
(8) Peigney, A.; Laurent, Ch.; Rousset, A. *J. Mater. Chem.* **1999**, *9*, 1167.
(9) Coquay, P.; De Grave, E.; Vandenberghe, R. E.; Dauwe, C.; Flahaut, E.; Laurent, Ch.; Peigney, A.; Rousset, A. *Acta Mater.* **2000**, *48*, 3015.
(10) Coquay, P.; Laurent, Ch.; Peigney, A.; Quenard, O.; De Grave, E.; Vandenberghe, R. E. *Hyperfine Interact.* **2000**, *130*, 275.
(11) Coquay, P.; Vandenberghe, R. E.; De Grave, E.; Fonseca, A.; Piedigrosso, P.; Nagy, J. B. *J. Appl. Phys.* **2002**, *92*, 1.
(12) Coquay, P.; De Grave, E.; Peigney, A.; Vandenberghe, R. E.; Laurent, Ch. *J. Phys. Chem. B* **2002**, *106*, 13186.
(13) Coquay, P.; Peigney, A.; De Grave, E.; Vandenberghe, R. E.; Laurent, Ch. *J. Phys. Chem. B* **2002**, *106*, 13199.
(14) Coquay, P.; De Grave, E.; Vandenberghe, R. E.; Peigney, A.; Laurent, Ch. *Hyperfine Interact.* **2002**, *139/140*, 289.
(15) Coquay, P.; Peigney, A.; De Grave, E.; Flahaut, E.; Vandenberghe, R. E.; Laurent, Ch. *J. Phys. Chem. B* **2005**, *109*, 17813.
(16) Coquay, P.; Flahaut, E.; De Grave, E.; Peigney, A.; Vandenberghe, R. E.; Laurent, Ch. *J. Phys. Chem. B* **2005**, *109*, 17825.
(17) Reshetenko, T. V.; Avdeeva, L. B.; Ushakov, V. A.; Moroz, E. M.; Shmakov, A. N.; Kriventsov, V. V.; Kochubey, D. I.; Pavlyukhin, Y. T.; Chuvilin, A. L.; Ismagilov, Z. R. *Appl. Catal., A* **2004**, *270*, 87.
(18) Kónya, Z.; Vesselényi, I.; Lázár, K.; Kiss, J.; Kiricsi, I. *IEEE Trans. Nanotechnol.* **2004**, *3*, 73.
(19) Bakandritsos, A.; Simopoulos, A.; Petridis, D. *Chem. Mater.* **2005**, *17*, 3468.
(20) Pérez-Cabero, M.; Taboada, J. B.; Guerrero-Ruiz, A.; Overweg, A. R.; Rodríguez-Ramos, I. *Phys. Chem. Chem. Phys.* **2006**, *8*, 1230.
(21) Prados, C.; Crespo, P.; González, J. M.; Hernando, A.; Marco, J. F.; Gancedo, R.; Grobert, N.; Terrones, M.; Walton, R. M.; Kroto, H. W. *Phys. Rev. B* **2002**, *65*, 113405.
(22) Marco, J. F.; Gancedo, J. R.; Hernando, A.; Crespo, P.; Prados, C.; González, J. M.; Grobert, N.; Terrones, M.; Walton, D. R. M.; Kroto, H. W. *Hyperfine Interact.* **2002**, *139/140*, 535.
(23) Ruskov, T.; Asenov, S.; Spirov, I.; Garcia, C.; Mönch, I.; Graff, A.; Kozhuharova, R.; Leonhardt, A.; Mühl, T.; Ritschel, M.; Schneider, C. M.; Groudeva-Zotova, S. *J. Appl. Phys.* **2004**, *96*, 7514.
(24) Lottermoser, W.; Schaper, A. K.; Treutmann, W.; Redhammer, G.; Tippelt, G.; Lichtenberger, A.; Weber, S. U.; Amthauer, G. *J. Phys. Chem. B* **2006**, *110*, 9768.
(25) Ruskov, T.; Spirov. I.; Ritschel, M.; Müller, C.; Leonhardt, A.; Ruskov, R.; *J. Appl. Phys.* **2006**, *100*, 084326.
(26) Ruskov, T.; Spirov, I.; Ritschel, M.; Müller, C.; Leonhardt, A.; Ruskov, R. *Bulg. J. Phys.* **2007**, *34*, 1.

(27) Seifu, D.; Hijji, Y.; Hirsch, G.; Karna, S. P. *J. Magn. Magn. Mater.*, in press.
(28) Jiang, L.; Gao, L. *Chem. Mater*. **2003**, *15*, 2848.
(29) Huiqun, C.; Meifang, Z.; Yaogang, L. *J. Solid State Chem*. **2006**, *179*, 1208.
(30) De Grave, E.; Vandenberghe, R. E.; Dauwe, C. *Hyperfine Interact*. **2005**, *161*, 147.
(31) Vandenberghe, R. E.; De Grave, E.; de Bakker, P. M. A. *Hyperfine Interact*. **1994**, *83*, 29.
(32) Dong, X. L.; Zhang, Z. D.; Xiao, Q. F.; Zhao, X. G.; Chuang, Y. C.; Jin, S. R.; Sun, W. M.; Li, Z. J.; Zheng, Z. X.; Yang, H. *J. Mater. Sci*. **1998**, *33*, 1915.
(33) Laurent, Ch.; Blaszczyk, Ch.; Brieu, M.; Rousset, A. *Nanostruct. Mater*. **1995**, *6*, 317.
(34) Larsson, L.; O'Neill, H. St. C.; Annersten, H. *Eur. J. Mineral*. **1994**, *6*, 39.
(35) Sethuraman, A. R. *Nanostruct. Mater*. **1994**, *4*, 79.
(36) Fung, K. K.; Qin, B.; Zhang, X. X. *Mater. Sci. Eng*. **2000**, *A286*, 135.
(37) Kuhn, L. T.; Bojesen, A.; Timmermann, L.; Nielsen, M. M.; Mørup, S. *J. Phys.: Condens. Matter*. **2002**, *14*, 13551.
(38) Cui, Z. L.; Dong, L. F.; Zhang, Z. K. *Nanostruct. Mater*. **1995**, *5*, 829.